NASA TECHNICAL MEMORANDUM

NASA TM X-71778

NASA TM X-71778

SUMMARY OF MODEL VTOL LIFT FAN TESTS CONDUCTED AT NASA LEWIS RESEARCH CENTER

by James H. Diedrich
Lewis Research Center
Cleveland, Ohio 44135

TECHNICAL PAPER to be presented at
Workshop on Prediction Methods for Jet V/STOL Propulsion Aerodynamics sponsored by the
Naval Air Systems Command
Arlington, Virginia, July 28-31, 1975

SUMMARY OF MODEL VTOL LIFT FAN TESTS CONDUCTED AT NASA LEWIS RESEARCH CENTER

by

James H. Diedrich

Lewis Research Center
National Aeronautics and Space Administration
Cleveland, Ohio

ABSTRACT

Early in this decade three model VTOL lift fan studies were conducted in the NASA Lewis Research Center's 9' x 15' V/STOL Wind Tunnel. The purpose of the tests was to obtain overall performance and influencing factors as well as detailed measurements of the internal flow characteristics. The first experiment consisted of crossflow tests of a 15-inch diameter fan installed in a two-dimensional wing. Tests were run with and without exit louvers over a range of tunnel speeds, fan speeds, and wing angle of attack. The wing was then used for a study of installation effects on lift fan performance. The model tested consisted of three 5.5-inch diameter tip-turbine driven model VTOL lift fans mounted chord-wise in the two-dimensional wing to simulate a pod-type array. Several inlet and exit cover door configurations and an adjacent fuselage panel were tested. For the third program, a pod was attached to the wing, and an investigation was conducted of the effect of design tip speed on the aerodynamic performance and noise of a 15-inch diameter lift fan-in-pod under static and crossflow conditions. Three single VTOL lift fan stages were designed for the same overall total pressure ratio but at three different rotor tip speeds. This paper will summarize the important aspects and the principal conclusions of all of these tests.

INTRODUCTION

During the late 1960's, three VTOL lift fan studies were conducted in the NASA Lewis Research Center's 9' x 15' V/STOL Wind Tunnel. The overall objective of all of these tests was to obtain overall and detailed aerodynamic performance of the lift fans in the transition flight regime (e.g., from engine supported flight during hover to conventional wing supported flight). This paper will summarize the important aspects and the principal conclusions of these tests.

The first experiment was derived from military applications and utilized the fan-in-wing concept. This experiment was modeled after the XV-5A research airplane. At the time, it was not known if a high pressure-ratio fan (e.g., P.R. = 1.3) would be able to perform adequately in the highly distorted flow field of transition flight. The principal objective of this experiment was to investigate the internal and overall aerodynamic performance of a fan-in-wing design. A model fan having a 15-inch diameter was used in this experiment.

Interest was next focused on civil VTOL applications. Civil VTOL transports were usually depicted with multiple lift fans installed close together in pods. Multiple fans were required to provide the necessary redundancy for safe operation in engine-out conditions. The second experiment, therefore, investigated the installation effects encountered in an array of three model fans installed in the same wing section used in the first experiment. The objectives were to study the individual fan performance in the array and determine the effects of cover doors and simulated fuselage and wing surfaces mounted in close proximity to the model fans. Three 5½-inch diameter model fans were used in this study.

Noise reduction was the next area emphasized in civil VTOL applications. Consequently, low-noise 15-inch diameter fans were designed and installed in a pod around the wing section used in the previous two experiments. The low noise features incorporated were a reduction in stage pressure ratio to around 1.2 and an increase in the spacing between the rotor and stator. Three stages were designed and built to permit investigation of a range of tip speeds and blade loading. Overall and internal aerodynamic performance were studied. Acoustic measurements of the three fan stages were also made.

APPARATUS AND TEST CONDITIONS

All of the experiments were conducted in the LeRC 9' x 15' V/STOL Wind Tunnel. The fan model assemblies were mounted in a 17% thick two-dimensional wing section that spanned the 9-foot dimension of the test section. The angle of attack of the wing could be varied between $\pm$ 15°, and the tunnel flow velocity was varied from 0 ft/sec (static conditions) to 240 ft/sec. Overall forces on the wing were measured

on a 3-component external balance. An auxilliary balance was mounted within the wing to permit measurement of the axial force on the fan module in each case. The fans contained extensive internal aerodynamic instrumentation in order to obtain detailed internal performance. The fan models were driven by turbines powered by compressed air. Additional details of the wind tunnel features and balance details can be found in references 1 and 2.

FAN-IN-WING TESTS

This experiment was the first test of the fan-in-wing apparatus and was basically exploratory. The overall objective was to establish the effect of the distorted flow environment during the transition flight regime on the thrust and internal aerodynamic performance of the model fan. Details of the apparatus and test results can be found in references 2 and 3.

Crossflow Problem

The distorted flow environment is termed crossflow and is depicted in figure 1. During the transition from engine supported flight to wing supported flight the fan must operate while the aircraft is moving forward at a velocity equal to V_∞. As shown, the flow is forced to turn rather abruptly as it enters the fan and the exit flow from the fan is deflected by the slip-stream. The test program was designed to investigate the effect of crossflow in the response of the fan stage to the distorted inflow and outflow conditions during transition. The crossflow environment generates high and low velocity regions on the inlet. In the plane of the fan, the combination of the fan rotation and the incoming flow to the fan produces a retreating and advancing condition on the fan blades as they rotate. In addition, the crossflow interaction influences the back-pressure at the fan exit.

Fan Assembly

The fan rotor was driven by a compact two-stage supersonic turbine located in the hub section of the assembly as shown in figure 2. This arrangement provided for coaxial exhaust streams. High-pressure air to drive the turbine was supplied through six equally-spaced 12%-thick struts spanning the fan passage. These struts also served as the structural support for the inner components of the assembly.

Specific fan stage design characteristics were: over-all pressure ratio, 1.28; corrected tip speed, 980 fps; corrected weight flow, 39.8 lb/sec ($M = 0.60$); inlet total pressure, 2116 lb/ft^2; inlet total temperature, 80^oF; exit static pressure, 2116 lb/ft^2; axial thrust, 810 lbs; and power input, 580 hp. The fan rotor blades were double

circular arc sections with aspect ratio of 2.6, hub-tip ratio of 0.463, and tip solidity of 1.25. The fan stator blades were NACA 65-series sections with aspect ratio of 3 and tip solidity of 1.0. The rotor diameter was 15 inches. Two 0.060-inch diameter damper wires were located on the rotor blades at 60% of the passage height from the hub to reduce blade vibration and prevent blade flutter in crossflow. The axial spacing between rotor and stator blades was approximately 0.5 rotor tip chords or about 0.75 inches. The inlet bellmouth was designed to avoid velocity peaks on the outer shroud during static (no crossflow) operation. The design method is discussed in reference 4.

At the exit, four louver vanes for aft flow deflection were attached to the wing with remote actuation from a vane chord position of -2.5° to $+40^{\circ}$ from the fan axis. The exit louvers were 8%-thick airfoil sections (NACA 63-series, 0.6 lift coefficient) with a solidity of 1.25 and aspect ratio of 3.3.

The model fan contained extensive internal and external instrumentation as shown in figure 2. Total pressures (P) and flow angles (β) were measured at the outlet of the rotor and stator as shown. In addition, total temperatures (T) were measured at the rotor outlet. Surface static pressures were measured on the external surfaces of the wing and along the internal flow passage. Three ½-inch long wall rakes were located on the forward half of the inlet upstream from the rotor leading edge. In all, approximately 450 individual measurements were made on this model.

The fan was mounted in a wing section as shown in figure 3. The wing spanned the 9-foot dimension of the test section as shown. The fan was located on the tunnel centerline on the 25% chord position of the wing. The wing also rotated about the 25% chord position for angle of attack variation.

Fan Pressure Ratio

The most noteable performance variations with crossflow obtained in this experiment occurred in the fan stage total pressure, the rotor outlet total pressure, and the fan thrust envelope. The fan stage total pressure ratio is shown in figure 4 where the average total pressure ratio is plotted against the crossflow velocity. Results are shown for 100% and 70% design tip speed. The data generally decrease monotonically as the crossflow velocity increases. For comparison, the ideal variation of total pressure ratio is also shown on the figure. The ideal variation was computed assuming complete recovery of the crossflow total pressure as it entered the fan and fixed fan pressure ratio. The deviation from ideal pressure ratio is greatest at the higher tip speed than at the lower tip speed. The effect of angle of attack was more pronounced for positive angles (nose-up attitude) as anticipated. The decline in total pressure ratio with increased crossflow velocity was due to changes in the fan operating point due to

decreases in back pressure and to additional losses caused by the effects of the flow distortion in the fan inlet.

The effects of crossflow variations on the distribution of internal flow are shown in figure 5. The measured rotor exit total pressure ratio and computed theoretical change in rotor incidence angle (from method of ref. 5) are plotted against the circumferential position around the fan or with the zero degree position being the most forward position relative to the airflow V_o. The distortion of the freestream flow in the inlet in crossflow tends to produce a circumferential variation in incidence angle on the fan rotor. The figure clearly depicts a corresponding variation cyclic of rotor exit total pressure ratio. The changes in incidence angle (Δi) produced the measured variations in total pressure ratio. As shown, the magnitude of the variations are increased as the crossflow velocity increases. The data also indicate a decrease in the mean value of rotor total pressure ratio with increasing crossflow velocity, as was observed at the stage exit (fig. 4).

Fan Thrust

The variation of fan stage total axial thrust displayed a trend similar to that shown for the stage total pressure and an approximate 10% reduction in thrust occurred from V_o = 0 to 200 ft/sec. Fan stage thrust is determined primarily by exit total pressure and mass flow rate. Since flow rate changed only little with crossflow, it appeared therefore, that the crossflow variation of stage thrust was the result primarily of the crossflow variation of exit total pressure ratio. It was also found that the fan exit louver angle had only a minor effect on the fan stage thrust variation over the entire test range of crossflow velocity. The resulting fall-off in fan performance was considered acceptable since actually less fan thrust would be required as forward velocity increases during transition.

In order to evaluate the relative contributing effects of inlet flow distortion and exit back pressure ratio on fan performance in crossflow, it was helpful to define a basic performance map of the fan stage. Such a stage map without crossflow was obtained by attaching a remotely-actuated throttling device to the rear surface of the fan. The outer member of the throttle contained a diffusing section to achieve the lower values of exit static pressure. A conical throttle plug was supported by a cylindrical member which was fastened to the hub section of the fan. The cylinder separated the turbine and fan exhausts. The static performance map was defined in terms of a thrust parameter (corrected fan thrust divided by inlet frontal area based on rotor tip diameter). The average duct exit static pressure ratio, p_e/p_o, was chosen as the independent variable because it provided a direct assessment of the fan stage back pressure for this fan design.

The static performance map (V_o = 0 ft/sec) of figure 6 shows the envelope of the data obtained using the exit louvers as well as the throttle plug. Data for 100% and 70% design tip speed are shown. A comparison between the basic range characteristics of the fan stage and the back pressure variation imposed by the louvers (or any other thrust vectoring or spoiling device) indicates the match between the fan stage and exit device.

The map of figure 6 clearly shows the overall effect of fan back pressure variations on fan stage static thrust (V_o = 0). Thrust vectoring with louvers at design speed tended to first increase and then decrease thrust. At lower levels of tip speed, fan stage thrust tended to decrease as back pressure was increased for all values of louver position. A relatively good operating match appears to have been achieved between the louvers and the fan stage for this particular configuration.

A fan thrust map in crossflow was determined and is also shown in figure 6 for zero wing angle of attack, V_o = 200 ft/sec, and 100% and 70% design tip speed. Locations corresponding to the various louver positions are also given on this curve. The crossflow curves appear to be similar in form to the static thrust variation. This was taken to indicate that the back pressure effect on fan stage thrust due to louver deflection in crossflow was essentially the same as that due to conventional outlet duct throttling. The figure shows two predominant effects of crossflow on fan thrust performance. First the fan operating point is shifted towards reduced values of duct exit static pressure ratio. Second the crossflow distortion reduces the thrust level and changes the shape of the map.

It was felt that the shape of the thrust map and the fan's response to crossflow distortion is unique to each fan design. Consequently, the crossflow performance of a fan stage could not be predicted with certainty from a static thrust map.

Summary

The general conclusions reached in this fan-in-wing experiment were that crossflow induced severe flow distortion which produced changes in fan internal performance and that crossflow reduced the fan back pressure which changed the fan operating point. Both of these effects gave rise to a reduction in thrust compared to the ideal variation. However, the overall thrust change with crossflow was not severe as to imply a serious detriment to aircraft transition operation.

MULTIPLE FAN INSTALLATION EFFECTS

The objective of this experiment was to study the effects of propulsion system installation on the performance of multiple VTOL model lift fans. The location of a lift fan on a V/STOL aircraft is expected to have a significant effect on fan performance. Furthermore, such installation variables as inlet and exit cover door design and location, fan proximity to the fuselage, and the proximity of other fans or engines are all likely to affect the thrust of individual fans during takeoff and landing and during the transition to fully-wingborne flight (crossflow case). A summary of the test set up and principal results are given in reference 6.

As an expedient follow-on to the previous fan-in-wing tests, a model consisting of three 5½-inch diameter tip-turbine driven model lift fans was mounted chordwise in the two-dimensional wing to simulate a pod-type array (fig. 7). Individual fan thrust performance was measured under static and crossflow conditions with inlet and exit cover doors of various designs installed on the basic model. Tests were also performed with a large panel simulating an airplane fuselage mounted next to the fans at two lateral positions. Fan performance was measured in terms of exit total and static pressures, speed, and gross thrust for each fan. The three-fan assembly was mounted on a load cell balance within the wing to provide a measurement of fan static thrust. Overall model lift, drag, and moment coefficients were also determined.

A thrust ratio was used to facilitate the comparison of the data presented herein. It is defined as:

$$\frac{\Delta (F/\delta)}{(F/\delta)_{ref}} = \frac{(F/\delta) - (F/\delta)_{ref}}{(F/\delta)_{ref}} \qquad (1)$$

where F/δ is the measured corrected thrust, and $(F/\delta)_{ref}$ is the reference value of corrected thrust. In this investigation the reference condition was chosen as the value of corrected fan thrust for zero crossflow and without inlet or exit doors (clean configuration).

Inlet and Exit Doors

Figure 8 shows the various inlet and exit cover doors tested. The butterfly doors were intended to simulate individual circular doors covering each fan. The doors were located on the side of the model or on the centerline of the model fans as shown.

Figure 9 shows the thrust ratio for the individual fans plotted against crossflow velocity. There was a significant variation in the thrust between the upstream and the downstream fan as shown. As indicated in the figure, the thrust of the upstream fan decreased, while

the thrust of the downstream fan increased slightly over the entire range of crossflow velocities tested. The upstream fan had the greatest thrust loss because the entering air is forced to turn more abruptly than in the case of the two downstream fans. There was less inlet flow distortion and an increase in fan weight flow for the successive fan locations in the downstream direction. This increase was due to a partial recovery of the momentum of the inlet airstream. Changing the angle of attack resulted in a relative increase in thrust level for each fan at negative angles of attack (nose down) and a relative decrease in thrust level at positive angles of attack. This behavior is consistent with the results from the experiments with the single fan-in-wing.

The effects of the inlet and exit cover doors are summarized on figures 10 and 11, respectively. The values of thrust ratio for each door configuration are plotted against crossflow velocity. For the inlet doors (fig. 10) the most noteable result was that 90° open doors resulted in lower thrust levels than the other door configurations. Evidently, decreasing the door opening angle increases the interference to the inflow to the fans. As shown on the figure, the 90° openings resulted in about a 15% loss of thrust while the other doors resulted in only about 10% thrust loss. There was also a modest increasing trend of thrust as crossflow velocity increased.

Figure 11 shows the data for the exit doors. There was little variation in thrust levels among the configurations tested. As shown on the figure, the exit doors resulted in about a 10% thrust loss over the full range of crossflow velocity. There was no definite trend of the thrust level with increasing crossflow velocity.

Fuselage Panels

In some V/STOL aircraft configurations, the lift fans might be installed in the wings or in pods adjacent to the fuselage. To obtain a measure of the effect of an adjacent fuselage on fan performance, a large panel was installed in close proximity to the fans. The fuselage simulator panel extended well out in front of and behind the fans, as well as slightly below the lower surface of the wing, as shown in figure 12. The height of the panel was about three fan bellmouth diameters above the upper surface of the wing. Static tests were run with and without an inlet cover door. The cover door, shown attached in figure 12 was a single rectangular panel one fan bellmouth diameter in height at an opening angle of 135° from the horizontal.

Data are presented in figure 13. The effect of proximity of the fuselage simulator panel to the fan on static thrust was significant. The thrust loss was around 8% when the fuselage simulator panel was closest to the fan (position A), and around 12% when the rectangular inlet cover door was added. Lateral movement of the fuselage simulator

panel to position B for both configurations had little effect on the static thrust ratio. A slight increase in thrust at high crossflow velocity was observed in all cases.

Summary

The simplified model performance data presented herein have provided a significant insight into possible thrust losses and thrust distributions in a multiple lift fan array caused by the presence of adjacent fans, inlet and exit cover doors, and adjacent fuselage panels. The measured thrust variations due to these installation effects were of a sufficient magnitude to warrant consideration in the determination of installed thrust for takeoff and for individual fan thrust control during transition.

On the basis of these results, several model fans with installation hardware (e.g., inlet cover doors and exit louvers) were provided to the NASA Langley Research Center. The model fans were used to study realistic installation effects on the overall aerodynamic characteristics of a complete VTOL transport aircraft model. The initial results are presented in reference 7 and are also included in these proceedings.

FAN-IN-POD TESTS

The emphasis of this investigation was to design and test low pressure-ratio fans to determine the effects of tip speed and loading on the aerodynamic and acoustic performance of a fan suitable for a fan-in-pod installation for a civil VTOL transport. Details of the experiment were reported in reference 8. This experiment used the identical turbine drive and wing section as for the earlier fan-in-wing experiment.

Fan Assembly

Three rotors were designed having design tip speeds of 700, 900 and 1050 ft/sec. Interaction noise between the rotor and stator was reduced by increasing the axial spacing between the rotor and stator to around 2.3 to 3.1 rotor tip chords, depending on the specific design. (The previous fan-in-wing stage had a rotor/stator spacing of only 0.5 rotor tip chords.) The thickness of the wing was increased locally around the fan to accommodate the increase in the axial dimension of the fan module. Figure 14 shows the modification to the wing mounted in the tunnel. This configuration was noted as the fan-in-pod to differentiate it from the earlier fan-in-wing experiment.

The rotor diameters of the three low-noise stages were kept at 15 inches. However, the stage design pressure ratio was reduced to 1.21

to be more indicative of low noise designs. (Reduced stage pressure ratios indicate reduced fan velocities causing reductions in fan noise.) The detail design values for each of the three fan stages is shown in Table 1. As noted in the headings on Table 1, the key features of the designs are the variation in tip speed and blade loadings. The low tip speed design has the highest blade loading and vice-versa. A common set of stators were used for each rotor design. The number of stator blades and the stator setting angles were varied as noted. All of the rotors incorporated an integral mid-span damper to prevent excess vibration and flutter of the fan blades.

Essentially the same instrumentation was used in this fan as was described in relation to the earlier fan-in-wing model (fig. 2). Provisions were made in this design to remove the rakes in the fan inlet and between the rotor and stator when making acoustic measurements.

Aerodynamic Performance

The performance of each fan stage along the static operating line closely matched their design values, however, the static thrust performance characteristics of each fan displayed distinctive features. Figure 15 shows the thrust parameter plotted against stage back pressure ratio. Data for each fan stage are shown for 100% and 70% design tip speed. At 100% design speed for an increase in back pressure ratio the trend of the thrust level of the 750, 900, and 1050 ft/sec stages respectively decreased, remained quite uniform, and increased. The same trends in thrust level were evident in the data at 70% design speed. The static performance characteristics of the three stages showed that essentially the same overall performance can be obtained for each of the three design rotor tip speeds along the stage operating line. However, if the fan is required to operate over a wide range of back pressure ratios, the resultant stage thrusts could be radically different. The 750 ft/sec highly loaded stage might have a much narrower range of operation than the 1050 ft/sec lightly loaded stage for above-ambient back pressure ratios.

The crossflow characteristics of the three rotor designs were similar to those described earlier in connection with the earlier fan-in-wing model. The crossflow distortion in the fan inlet produced cyclic changes in rotor total pressure ratio as a function of circumferential position. Each rotor design had a unique reponse to crossflow indicating that each design would have a unique fan stage crossflow thrust characteristic.

Figure 16(a) shows a comparison of the variation of stage thrust parameter as tunnel airflow (crossflow) velocity is increased for the undeflected louver configuration at zero wing angle of attack. Two

principal observations can be made. The first is that, in general, there was no large fall-off in thrust as crossflow velocity was increased. Thus, the performance of the fan stages should pose no problems for lift fan operation during transition. The second observation is an apparent divergence of the thrust variations in crossflow for the three stage designs. The thrust in crossflow for the high-loading 750 ft/sec stage was always greater than that for the low-loading 1050 ft/sec stage, with the 900 ft/sec stage falling in between. Thus, as far as open-louver performance in crossflow is concerned, fan stage performance is again acceptable, with only small differences appearing for the three rotor design tip speeds.

Also plotted on figure 16(b) are the corresponding values of stage back pressure ratio from the static thrust for the individual fan stages. Crossflow produces a tendency for the fan operating point to shift toward lower values of back pressure ratio. Thus the static data shown tend to support the variation trends with crossflow velocity.

Additional tests performed varying the louver angle in crossflow produced variations in stage thrust were similar to the individual variations of static thrust with back pressure ratio. The data indicated lower design tip speed stages showed more favorable thrust variation for moderate louver deflection angles while the higher tip speed designs appeared better for very large deflection angles. Further details are given in reference 8.

Acoustic Results

The acoustic measurements were made in the tunnel under static conditions. Results were reported in reference 9. Figure 17 shows the locations of the microphones in the tunnel. Four microphones were located upstream and downstream from the test section as shown. The acoustic installation was designed to approximate a reverberant sound chamber where the sound pressure level was essentially uniform throughout the enclosure. For the static noise tests, the wing was turned with its chord normal to the axis of the test section. The upstream microphones were used when the fan inlet was facing upstream. All data presented are forward radiated values.

For the noise measuring tests, a silencer was attached directly to the exit of the drive turbine. The purpose of this silencer was to reduce the turbine exhaust velocity and absorb some of the internally generated turbine noise, so that the fan stage noise content could be isolated. Details of the silencer design are given in reference 9.

Figure 18 shows narrow band spectra for the three rotor designs recorded at 100% fan design speed. Again, each fan design displayed unique characteristics. The appearances of the spectra became more ragged in appearance progressing from the 750 ft/sec design to the

1050 ft/sec design. The sound pressure level at the blade passing frequency (point F) were essentially identical, however, the balance of the curves were distinctly different among the three designs. The 1050 ft/sec design stage displayed a large amount of multiple pure tone noise (sharp peaks). The multiple pure tones produce a "buzz saw" noise and are associated with the irregular shock patterns formed by the transonic flow relative to the fan blade.

The principal aerodynamic design parameters believed to be related to the fan stage noise generation are: (a) the total pressure rise (measure of specific work input to the air); (b) the relative inlet Mach number in the rotor tip region (measure of multiple-pure-tone and broadband noise generation); and (c) blade loading (measure of wake formation and interaction noise). In an attempt to factor out these parameters comparison plots were made for the noise (PWL) of the three stages against rotor tip relative inlet Mach number and stage total pressure rise ratio (pressure ratio minus one). The PWL values were obtained from the spectral measurements shown previously.

Figure 19 shows that the subsonic design stages (750 and 900 fps) tended to produce a leveling off in forward radiated power level as tip relative inlet Mach number was increased to around 1.05. Beyond that value, there was an increase in power level. A sharp rise in power level is especially pronounced for the 1050-fps stage beyond a tip relative inlet Mach number of around 1.0. As indicated previously, these increases in noise power were the result of the appearance of multiple pure tone noise due to irregular shock wave formations at the rotor inlet.

At a given tip relative inlet Mach number below the "critical" value (i.e., formation of MPT noise), the sound power level tended to decrease with increasing rotor design tip speed. However, it should be noted that both total pressure ratio and blade loading also decrease with increasing rotor design tip speed for a given tip relative inlet Mach number. It is, therefore, necessary to examine the corresponding plots of forward-radiated power level versus total pressure rise ratio as shown in figure 13.

The variations of figure 20 tend to suggest the existence of "subsonic" and "supersonic" noise trends. The 750-fps stage results and the low-pressure rise values for the 900- and 1050-fps stages can be interpreted to represent a basic subsonic correlation in terms of pressure rise. In this region, it appears that blade loading may be a significant parameter, inasmuch as the highest design tip speed stage[1] tended to produce the lowest noise level despite its higher tip relative Mach number. The attainment of the same power level for

(1) It should be noted that the 1050-fps stage also had the largest effective separation distance between rotor and stator as indicated in Table 1.

the 750- and 900-fps designs at their design tip speed may have been due to a counter-balancing of the relative velocity and blade loading effects in these two stages.

Summary

The general conclusions reached in this fan-in-pod experiment were the aerodynamic performance of the three fan stage designs attained their static design performance goals, and crossflow performance was good at the design point. The static thrust maps had significant variations between the three designs. The 750 ft/sec design (highest aerodynamic loading) had the smallest stall margin while the 1050 ft/sec design (lowest aerodynamic loading) had the widest stall margin. The crossflow aerodynamic performance for the three designs were equally unique. However, back pressure changes significantly changed the fan operating point for each design and the inlet distortion changes were not significant.

The acoustic performance of each fan was also unique. The sound power level for the three stages appeared to be composed of a "subsonic" and a "supersonic" trend. These trends were dependent on tip speed and possibly blade loading.

It is apparent that in order to obtain the best matched lift fan for a particular application, the installation (back pressure effects) should be tailored to the fan performance map characteristics. It is also necessary to be able to predict the back pressure variation in crossflow.

CONCLUDING REMARKS

The research tests on model lift fans described herein provided a valuable understanding of the performance variations and flow behavior of lift fans during the transition from vertical to wing-borne flight. Principal performance trends were established, primary influencing factors were identified, and the importance of installation effects on fan performance was documented. Finally, the program demonstrated that lift fans can be designed to operate satisfactorily in the distorted flow environment induced by forward velocity during transition. A necessary ingredient in this design procedure is a method for calculating the potential and viscous flow in the inlet of the fans. Such a method is described in a companion paper.

REFERENCES

1. Yuska, J. A.; and Diedrich, J. H.: Lewis 9- By 15-Foot V/STOL Wind Tunnel. NASA TM X-2305, July 1971.

2. Yuska, J. A. ; and Diedrich, J. H.: Fan and Wing Force Data from Wind-Tunnel Investigation of a 0.38-Meter (15-Inch) Diameter VTOL Model Lift Fan Installed in a Two-Dimensional Wing. NASA TN D-6654, March 1972.

3. Lieblein, S.; Yuska, J. A.; and Diedrich, J. H.: Performance Characteristics of a Model VTOL Lift Fan in Crossflow. Journal of Aircraft, Vol. 10, No. 3, March 1973, pp. 131-136.

4. Stockman, N. O.; and Lieblein, S.: Theoretical Analysis of Flow in VTOL Lift Fan Inlets Without Crossflow. NACA TN D-5605, Feb. 1969.

5. Stockman, N. O.: Potential Flow Solutions for Inlets of VTOL Lift Fans and Engines. Analytic Methods in Aircraft Aerodynamics, NASA SP-228, Washington, D.C., 1970, pp. 659-681.

6. Diedrich, J. H., Clough, N.; and Lieblein, S.: Installation Effects on Performance of Multiple Model V/STOL Lift Fans. Journal of Aircraft, Vol. 10, No. 6, June 1973, pp. 355-360.

7. Hoad, D. R.; and Gentry, G. L., Jr.: Longitudinal Aerodynamics of a Low-Wing Lift-Fan Transport Including Hover Characteristics In and Out of Ground Effect. NASA TM X-72670, April, 1975.

8. Stockman, N. O.; Loeffler, I. J.; and Lieblein, S.: Effect of Rotor Design Tip Speed on Aerodynamic Performance of a Model VTOL Lift Fan Under Static and Crossflow Conditions. Journal of Engineering for Power, Trans. ASME, October 1973, pp. 293-300.

9. Loeffler, I. J.; Lieblein, S.; and Stockman, N. O.: Effect of Rotor Design Tip Speed on Noise of a 1.21 Pressure Ratio Model Fan Under Static Conditions. ASME Paper No. 73 WA/GT-11, Nov. 1973.

TABLE I. - FAN STAGE DESIGN VALUES (UNSHROUDED ROTORS)

1.21 PRESSURE RATIO

Features	Low tip speed, high loading	Medium tip speed, medium loading	High tip speed, low loading
ROTOR			
Corrected tip speed, ft/sec	750	900	1050
Relative tip inlet Mach no. [a]	0.88	0.99	1.10
Number of blades	37	37	34
Tip solidity	1.1	1.1	1.0
Tip diffusion factor [a]	0.41	0.34	0.32
Maximum tip thickness/chord	0.05	0.05	0.04
Maximum hub thickness/chord	0.08	0.08	0.08
STATOR			
Relative hub inlet Mach no. [a]	0.68	0.62	0.59
Number of blades	42	42	36
Tip solidity	1.1	1.1	0.94
Hub diffusion factor [a]	0.42	0.33	0.29
Stagger angle reset, deg	+3	0	-2.5
Maximum tip thickness/chord	0.07	0.07	0.07
Maximum hub thickness/chord	0.06	0.06	0.06
Stage efficiency	0.86	0.86	0.83
Rotor-stator axial spacing [b]	2.3	2.8	3.1

[a] At 5 percent of span from wall.
[b] In projected rotor tip chords.

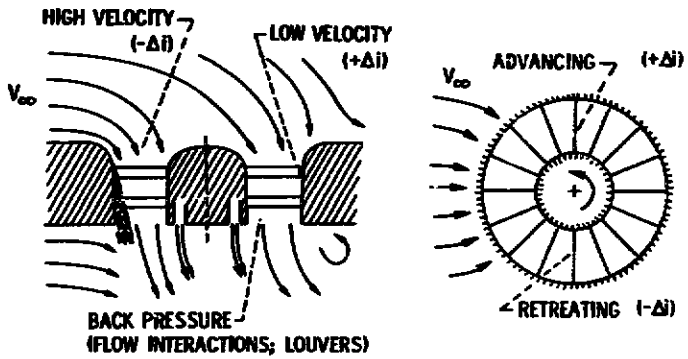

CS-56232

Figure 1. - Lift fan inflow in crossflow.

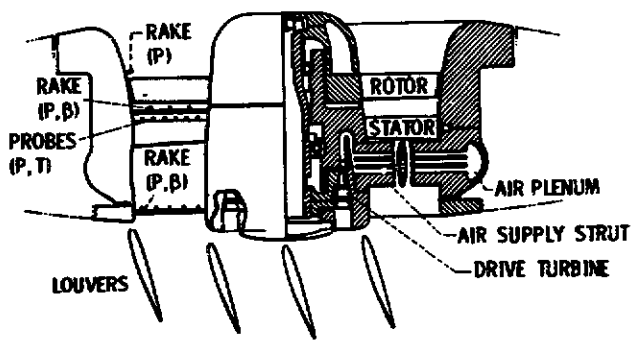

Figure 2. - Cross section of 15-in. model lift fan.

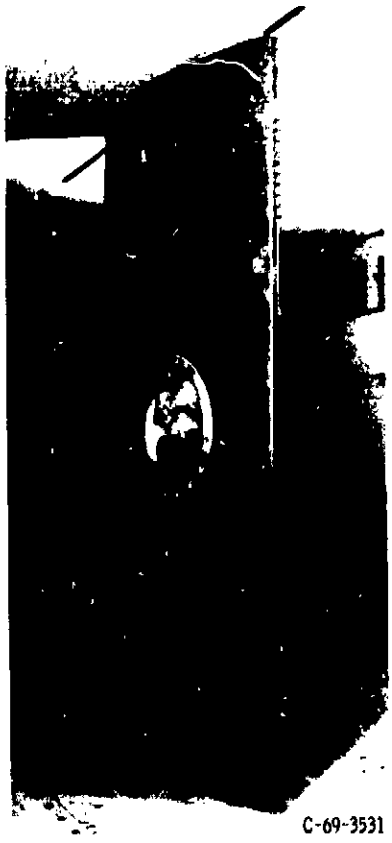

C-69-3531

Figure 3. - The 15-in.-diameter fan-in-wing model installed in the Lewis Research Center 9 by 15 ft V/STOL test section.

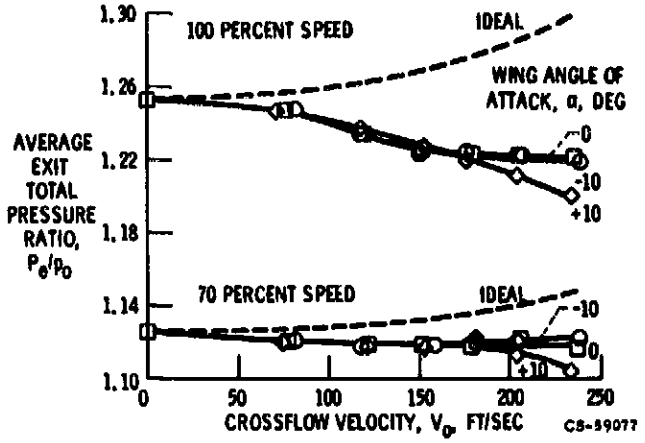

Figure 4. - Fan duct exit total pressure ratio crossflow - louvers off.

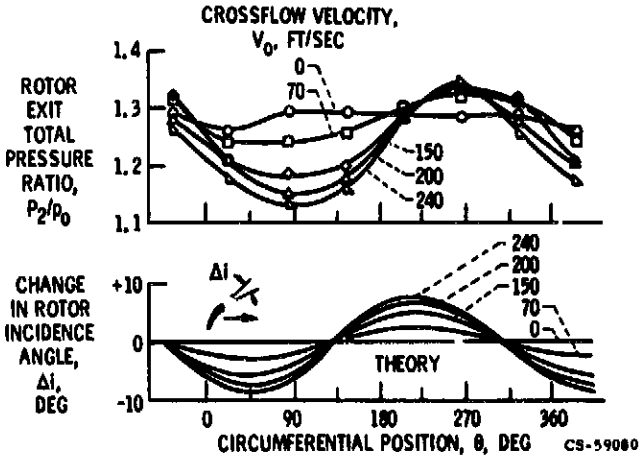

Figure 5. - Rotor outlet total pressure in crossflow - midpassage radius; design speed.

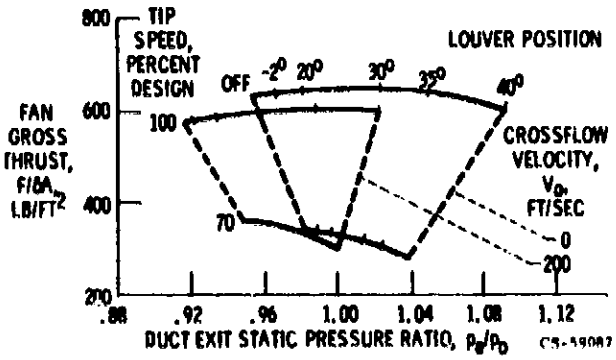

Figure 6. - Fan thrust envelope - zero angle of attack.

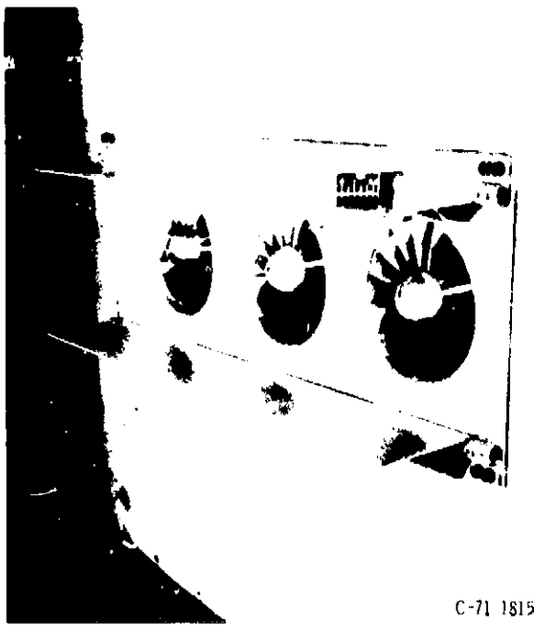

(a) RECTANGULAR SIDE DOORS, 90° OPEN POSITION.

(b) SIDE SCOOP BUTTERFLY DOORS, 135° OPEN POSITION.

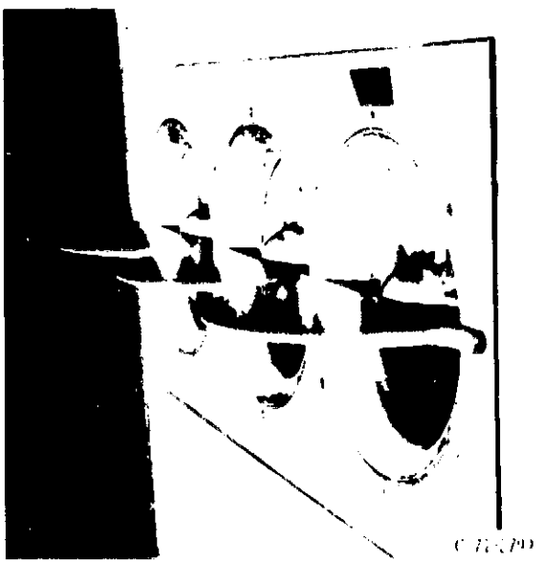

(c) CENTER BODY BUTTERFLY DOORS.

(d) [illegible]

Figure [illegible]

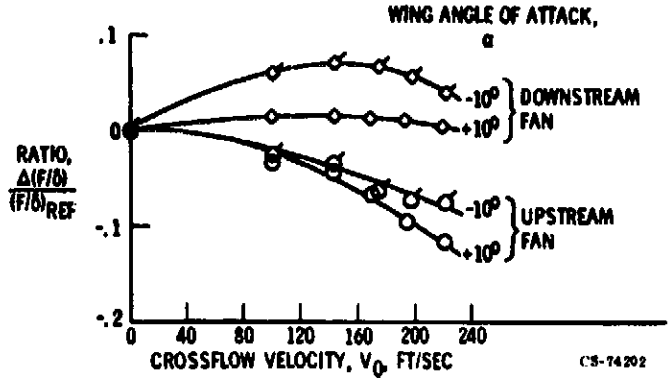

Figure 9. - No inlet or exit doors, range of angle of attack. Variation in thrust for each fan with crossflow velocity. All three fans running at 100 percent $N/(\theta)^{1/2}$.

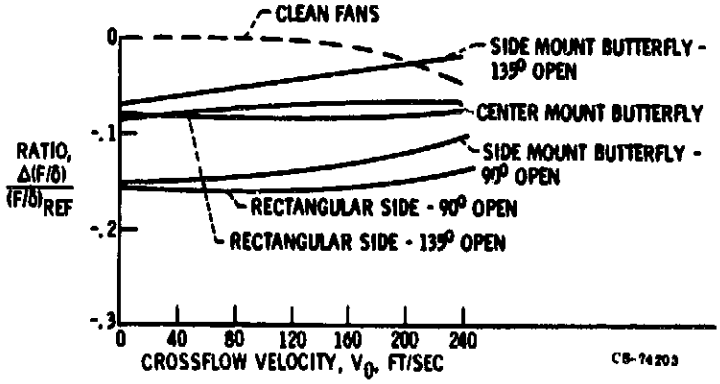

Figure 10. - Variation in thrust with crossflow velocity for various inlet door configurations. All three fans running at 100 percent $N/(\theta)^{1/2}$, $\alpha = 0^{\circ}$.

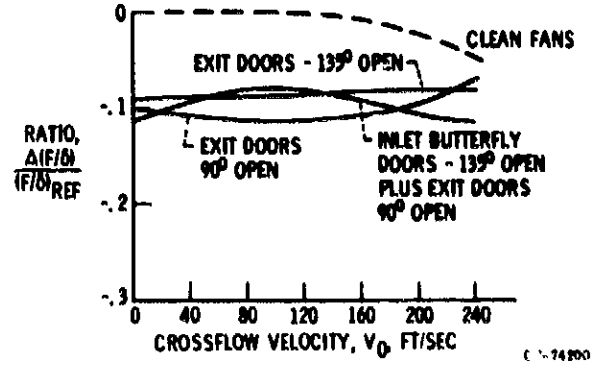

Figure 11. - Variation in thrust with crossflow velocity for various rectangular exit door configurations. All three fans running at 100 percent $N/(\theta)^{1/2}$, $\alpha = 0^{\circ}$.

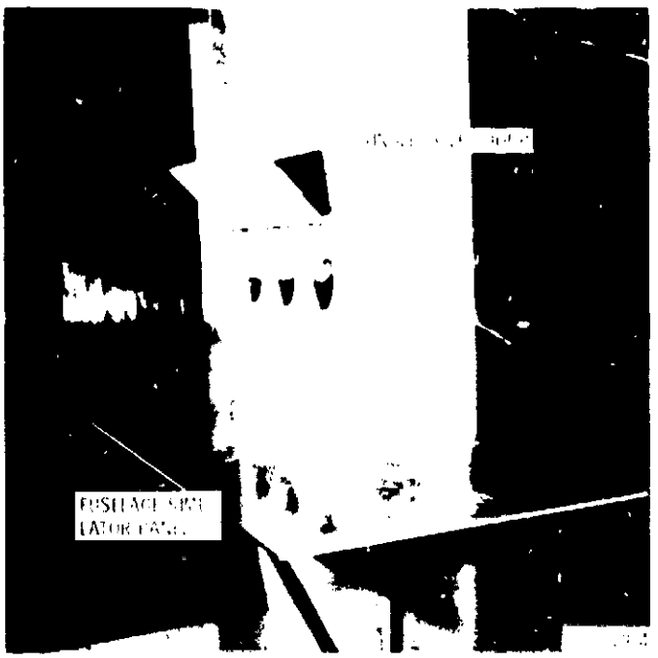

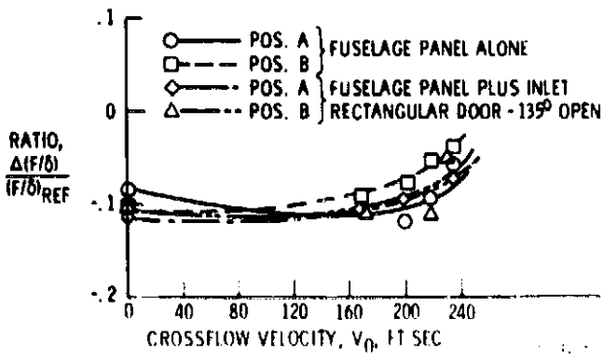

Figure 13. - Variation in thrust with crossflow velocity for various fuselage panel configurations. All three fans running at 100 percent $N/\theta^{1/2}$; $\alpha = 0^{\circ}$.

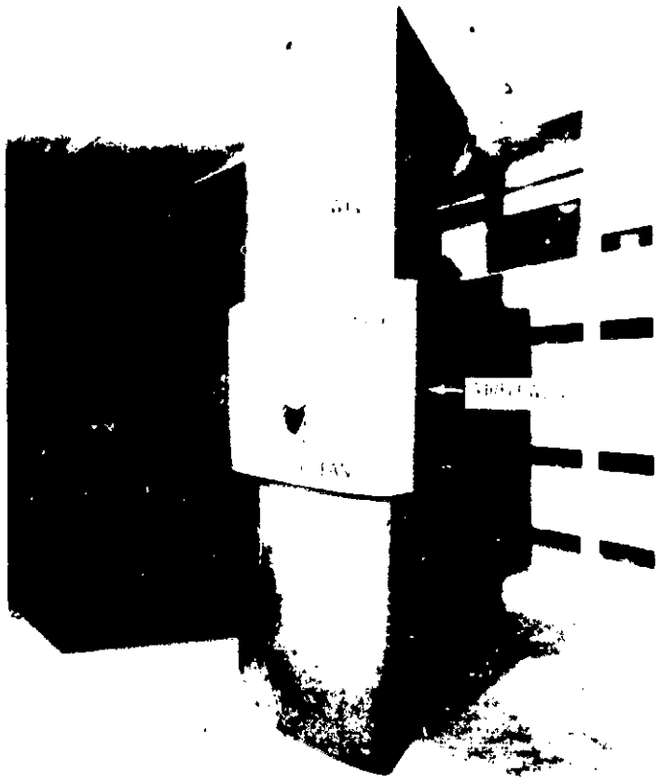

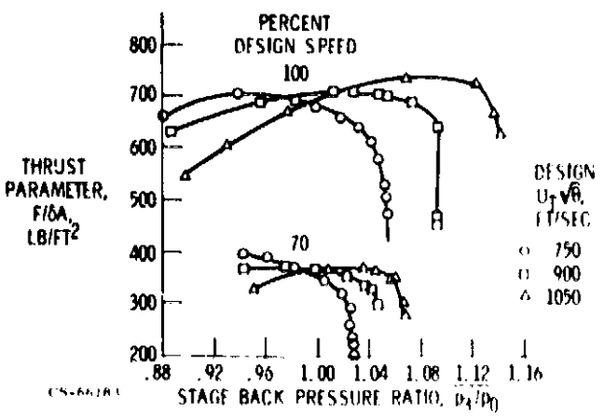

Figure 15. Fan stage static thrust maps obtained from throttle duct tests.

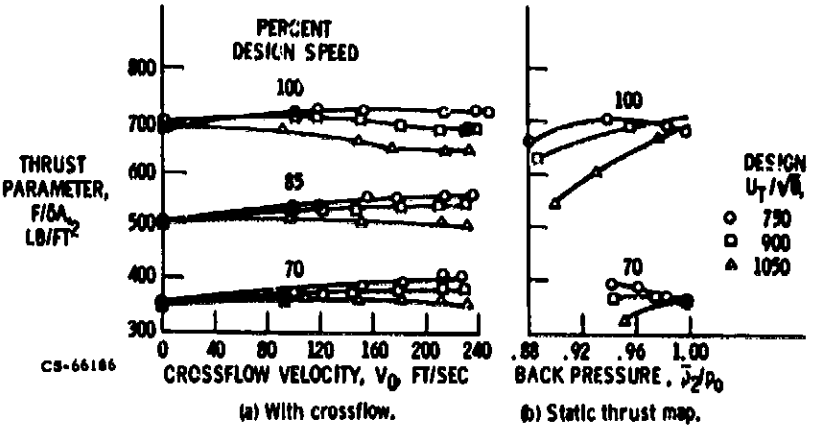

Figure 16. - Variation of fan stage thrust. Louver angle, $\beta_L = 0.5^0$; wing angle, $\alpha = 0^0$.

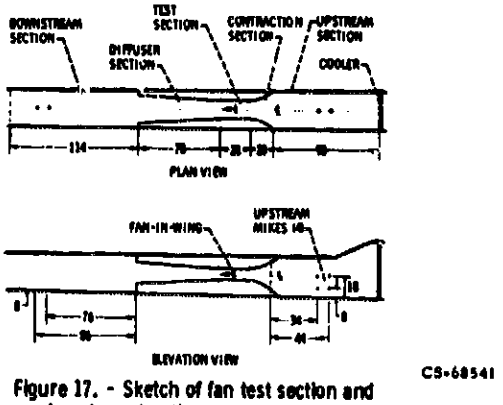

Figure 17. - Sketch of fan test section and microphone locations; Lewis 9- x 15-ft V/STOL wind tunnel. All dimensions in feet.

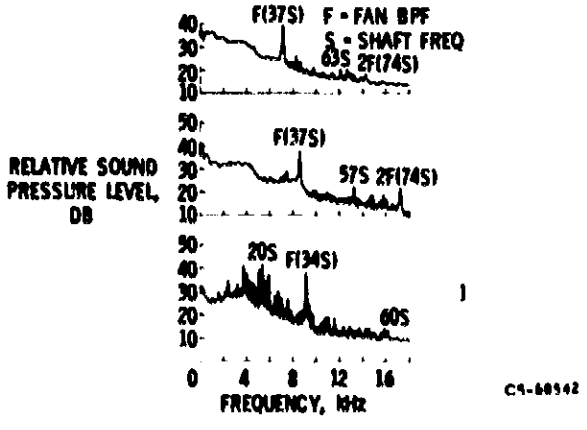

Figure 18. - Narrow band spectra at 100 percent design speed. Forward radiated noise.

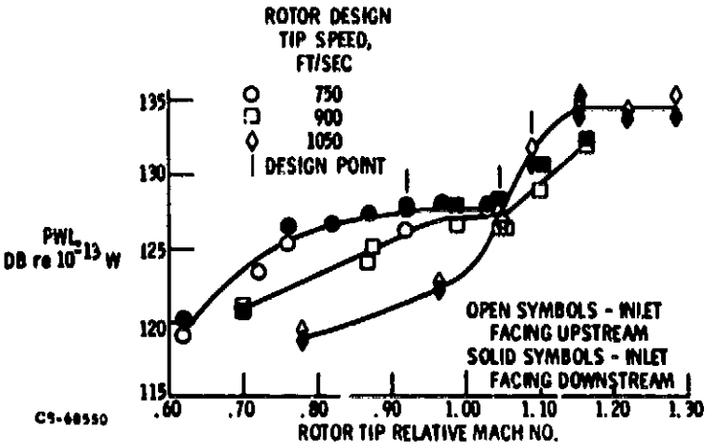

Figure 19. - Forward radiated sound power versus relative inlet Mach number at rotor tip.

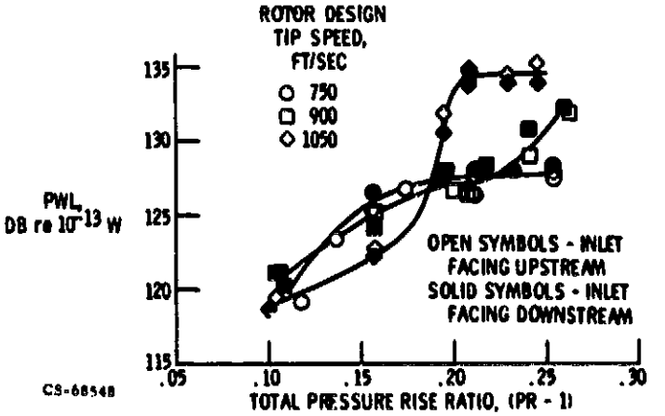

Figure 20. - Forward radiated sound power versus pressure rise ratio for three 1.21 stage pressure ratio fans.